THE JOURNAL OF BIOLOGICAL CHEMISTRY VOL. 286, NO. 42, pp. 36361–36367, October 21, 2011

Local Elongation of Endothelial Cell-anchored von Willebrand Factor Strings Precedes ADAMTS13 Protein-mediated Proteolysis*[S]

Received for publication, June 16, 2011, and in revised form, August 22, 2011 Published, JBC Papers in Press, September 6, 2011, DOI 10.1074/jbc.M111.271890

Karen De Ceunynck[‡1], Susana Rocha[§], Hendrik B. Feys[‡2], Simon F. De Meyer[‡3], Hiroshi Uji-i[§], Hans Deckmyn[‡], Johan Hofkens[§4], and Karen Vanhoorelbeke[‡5]

From the [‡]Laboratory for Thrombosis Research, Katholieke Universiteit Leuven Campus Kortrijk, B-8500 Kortrijk and the [§]Division of Molecular and Nano Materials, Department of Chemistry, Katholieke Universiteit Leuven, B-3001 Leuven, Belgium

Platelet-decorated von Willebrand factor (VWF) strings anchored to the endothelial surface are rapidly cleaved by ADAMTS13. Individual VWF string characteristics such as number, location, and auxiliary features of the ADAMTS13 cleavage sites were explored here using imaging and computing software. By following changes in VWF string length, we demonstrated that VWF strings are cleaved multiple times, successively shortening string length in the function of time and generating fragments ranging in size from 5 to over 100 μm. These are larger than generally observed in normal plasma, indicating that further proteolysis takes place in circulation. Interestingly, in 89% of all cleavage events, VWF strings elongate precisely at the cleavage site before ADAMTS13 proteolysis. These local elongations are a general characteristic of VWF strings, independent of the presence of ADAMTS13. Furthermore, large elongations, ranging in size from 1.4 to 40 μm, occur at different sites in space and time. In conclusion, ADAMTS13-mediated proteolysis of VWF strings under flow is preceded by large elongations of the string at the cleavage site. These elongations may lead to the simultaneous exposure of many exosites, thereby facilitating ADAMTS13-mediated cleavage.

von Willebrand factor (VWF)[6] is a large multimeric glycoprotein that plays an important role in hemostasis (1). Apart from serving as a protecting carrier for factor VIII, the main function of VWF is mediating initial platelet adhesion to the damaged vessel wall by forming a bridge between subendothelial collagen and platelets in circulation (2–4). VWF is synthesized by endothelial cells (EC) and megakaryocytes as a multimeric protein ranging in size from 500 to more than 20,000 kDa (2, 5). VWF is secreted in blood either constitutively or upon stimulation from Weibel-Palade bodies in EC or from α-granules in platelets. Stimulation of EC results in the release of ultra-large (UL), hyper-reactive VWF multimers (>20,000 kDa), some of which remain attached to the endothelial surface. If unprocessed, these UL-VWF multimers can spontaneously bind and agglutinate platelets generating widespread microthrombi in circulation, leading to thrombotic thrombocytopenic purpura (6–8). In normal hemostasis, UL-VWF multimers are rapidly cleaved by ADAMTS13 (a disintegrin and metalloproteinase with a thrombospondin type-1 motif, member 13) into smaller but still hemostatically active multimers (9). The interaction between ADAMTS13 and VWF occurs through a unique mechanism that involves conformational changes in VWF. The scissile bond in the VWF A2 domain (Tyr-1605–Met-1606 bond) is cryptic in the folded VWF molecule and only becomes accessible for ADAMTS13 proteolysis when VWF undergoes a conformational change (10, 11).

In the absence of ADAMTS13, UL-VWF multimers decorated with platelets (VWF strings) persist on the endothelial surface both *in vitro* and *in vivo* for several minutes (12, 13). Interestingly, only a subset of VWF strings is decorated with platelets. These VWF strings can form bundles or networks and seem to be attached to the endothelial surface through a limited number of sites (14). Anchorage through both P-selectin and $\alpha v\beta 3$ has been reported *in vitro* (14, 15), although this has not been confirmed *in vivo* (16). In the presence of active ADAMTS13, VWF strings are rapidly cleaved once or twice near the upstream attachment sites (12). ADAMTS13 also cleaves EC-anchored VWF in the absence of shear and platelets (17, 18), demonstrating that under these conditions, the scissile bond in the VWF A2 domain must be accessible. Furthermore, no difference was observed in the rate of ADAMTS13 cleavage between platelet-free and platelet-decorated VWF strings under a shear stress of 2.5 dyne/cm^2 (14).

Previous experiments on endothelium-derived and freshly released VWF multimers, however, did not elaborate on individual string characteristics such as the location of ADAMTS13

* This work was supported by grants from the Research Foundation Flanders (Fonds voor Wetenschappelijk Onderzoek Vlaanderen (FWO)) (Grants G.0299.06, G.0607.09, G.0402.09, and G0603.10) and the Katholieke Universiteit Leuven (K.U.Leuven) (Grants GOA/2004/09 and GOA/2011/03).

[S] The on-line version of this article (available at http://www.jbc.org) contains supplemental Figs. S1–S4.

[1] Supported by a Ph. D. grant Agentschap voor Innovatie door Wetenschap en Technologie (IWT number 83328) of the Institute for the Promotion of Innovation through Science and Technology in Flanders (IWT-Vlaanderen).

[2] A fellow of the Special Research Fund of the K.U.Leuven.

[3] A fellow of the FWO.

[4] To whom correspondence may be addressed: Division of Molecular and Nano Materials, Dept. of Chemistry, Katholieke Universiteit Leuven, Celestijnenlaan 200F, B-3001 Leuven, Belgium. Tel.: 32-16-32-78-04; Fax: 32-16-32-79-90; E-mail: johan.hofkens@chem.kuleuven.be.

[5] To whom correspondence may be addressed: Laboratory for Thrombosis Research, Katholieke Universiteit Leuven Campus Kortrijk, E. Sabbelaan 53, B-8500 Kortrijk, Belgium. Tel.: 32-56-24-60-19; Fax: 32-56-24-69-97; E-mail: karen.vanhoorelbeke@kuleuven-kortrijk.be.

[6] The abbreviations used are: VWF, von Willebrand factor; ADAMTS13, a disintegrin and metalloproteinase with a thrombospondin type-1 motif, member 13; EC, endothelial cells; BOEC, blood outgrowth endothelial cell; UL, ultra-large; DIOC6, 3,3′-dihexyloxacarbocyanine iodide.

cleavage sites, the number of events in a given string, and auxiliary features enhancing or promoting the probability of proteolysis. Therefore, we developed and used imaging and computing software that now allows rigorous analysis to address these questions. We show here that VWF strings are gradually shortened in the function of time by multiple cleavage events and that ADAMTS13-mediated cleavage occurs at sites in VWF that undergo large elongations.

EXPERIMENTAL PROCEDURES

Blood Sample Collection

Blood was drawn from healthy volunteers who gave informed consent. The study was approved by the Institutional Clinical Review Board of the Katholieke Universiteit Leuven (Leuven, Belgium) and performed according to the Declaration of Helsinki.

Preparation of Washed Platelets

Blood was drawn on acid-citrate-dextrose (85 mM sodium citrate, 111 mM glucose and 71 mM citric acid, pH 4.5, 10% v/v) and centrifuged at 120 × *g* for 15 min at room temperature to obtain platelet-rich plasma. The platelet-rich plasma was supplemented with apyrase (75 microunits/ml; Sigma-Aldrich) and prostaglandin E_1 (100 nM; Sigma-Aldrich) and centrifuged for 15 min at 1200 × *g*. The platelet pellet was resuspended in wash buffer (36 mM citric acid, 5 mM glucose, 5 mM KCl, 1 mM $MgCl_2$, 103 mM NaCl, 2 mM $CaCl_2$, 75 microunits/ml apyrase, 100 nM PGE1, 3.5 mg/ml bovine serum albumin, pH 6.5) and centrifuged for 12 min at 1200 × *g*. Finally, the platelet pellet was resuspended in Hepes/Tyrode's buffer (137 mM NaCl, 2 mM KCl, 3 mM NaH_2PO_4, 1 mM $MgCl_2$, 5.5 mM glucose, 5 mM Hepes, 12 mM $NaHCO_3$, pH 7.4), and the washed platelets were used at a platelet count between 20,000 and 30,000 platelets per μl.

Endothelial Cell Culture

Blood outgrowth endothelial cells (BOECs) were isolated from human healthy volunteers and characterized by immunofluorescent microscopy as described previously (19, 20). BOECs (passages 2–6) were grown on collagen-coated cover slides in EBM-2/EGM-2 culture medium (Lonza, San Diego, CA) as described (19, 20).

Recombinant ADAMTS13 Production and Purification

Human recombinant wild-type (WT) ADAMTS13 and inactive mutant ADAMTS13 (E225Q) (gift from Dr. Sadler, St. Louis, MO) were expressed using an inducible T-Rex system (Invitrogen). Conditioned medium containing recombinant ADAMTS13 was adsorbed on a heparin-Sepharose column (GE Healthcare). After washing with 50 mM MES buffer, pH 6.6, ADAMTS13 was eluted with 50 mM MES, pH 6.6, containing 1 mM NaCl. Fractions were pooled, concentrated, and dialyzed against Hepes-buffered saline solution (50 mM HEPES, pH 7.4, 5 mM $CaCl_2$, 1 mM $ZnCl_2$, and 150 mM NaCl) as described (21). Concentrations were determined using a sandwich ELISA with normal human pooled plasma ($n = 20$) as a reference. Purity was estimated by SDS-PAGE with subsequent SimplyBlue™ staining (Invitrogen) (8, 21). Enzyme activity was measured using the fluorogenic FRETS-VWF73 substrate (Peptides International, Louisville, KY) as described previously (22, 23).

Visualization of ADAMTS13-mediated VWF Cleavage on the Surface of BOECs in a Parallel-plate Flow Chamber

The formation and cleavage of BOEC-anchored VWF strings were studied in a parallel-plate flow chamber as described (12). The flow chamber was developed in-house and consists of two metal plates, a polydimethylsiloxane gasket, and a coverslip (24 mm wide by 40 mm long, Menzel-gläser, Thermo Fisher Scientific). Briefly, BOECs were grown on a collagen-coated coverslip until confluent and stimulated with 25 μM histamine (Sigma-Aldrich) for 10 min at room temperature. Next, coverslips were mounted in the parallel-plate flow chamber and were subsequently perfused with fluorescently labeled (100 nM 3,3′-dihexyloxacarbocyanine iodide (DIOC6), Invitrogen) washed platelets at a shear rate of 250 s^{-1} causing a shear stress of 2.5 dynes/cm^2 for a duration of 105 s. Flow rate was adjusted with a syringe pump (Harvard Apparatus, Holliston, MA). After perfusion with platelets, the coverslip was perfused with Hepes-buffered saline buffer with or without ADAMTS13 (25 nM) for an additional 135 s. In control experiments, ADAMTS13 was preincubated with the inhibitory monoclonal antibody (mAb) 3H9 (67 nM) (24). DIOC6-labeled platelets were excited with a mercury lamp at wavelengths between 450 and 490 nm (band pass filter, 470 center wavelength) visualizing platelet-decorated VWF strings in real time with an Eclipse TE200 inverted fluorescence microscope (objective 20×, 0.4 NA) (Nikon Instruments, Melville, NY) coupled to a Hamamatsu CCD camera (ORCA®-R^2, Hamamatsu Photonics, Hamamatsu City, Japan). Videos (frame rate 1/0.15 s^{-1}) were recorded using the Hokawo software (Hamamatsu Photonics) for 240 s starting 60 s after the initiation of flow. A bulk study of cleavage of VWF strings by ADAMTS13 was performed by arbitrarily selecting 20 VWF strings in one view field and following the remainder of selected strings every 10 s. The mean and S.E. were calculated for data from three independent experiments.

Image Processing and Identification of Fluorescently Labeled Platelets

A detailed analysis of cleavage of individual VWF strings by ADAMTS13 was performed to determine the number, location, and specific characteristics of the cleavage sites. Therefore, images acquired in the presence of active ADAMTS13, inactive ADAMTS13 (E225Q), or buffer were analyzed using a routine developed in-house in Matlab®, based on the detection of fluorescently labeled platelets. After adequate image filtering processes (smoothing), the first frame of each movie (taken 60 s after the start of each experiment) (supplemental Fig. S1*A*) was converted into a binary image, using an adjustable threshold for platelet recognition (supplemental Fig. S1*B*). In this way, platelets were selected automatically, the centroid (geometric center) of such selected platelets was determined, and the periphery of each cell was encircled (supplemental Fig. S1, *C* and *D*, *green dots*, and *E*, *green circles*). Next, VWF strings (larger than 20 μm and having at least three platelets bound to them) were arbitrarily chosen for each movie by manually selecting the first

and last platelet of the VWF string (supplemental Fig. S1*D*). Using the same image processing steps as for the initial image, each selected string and the surrounding area (14 μm at the sides and an additional 105 μm before and after the selected string) were then analyzed for all remaining frames (1200) of the movie. Afterward, all frames could be manually corrected to add non-detected platelets and delete background spots that were falsely identified as platelets. VWF strings were rejected from analysis when the VWF string was out of focus, too close to other VWF strings, or detached because of the drag caused by attachment of another string (self-association of VWF strings). Supplemental Fig. S1*E* shows a representative VWF string with automatically selected platelets.

VWF String Analysis and Cleavage by ADAMTS13

Determining the Number of Platelets per VWF String—After manual correction, the software calculated the number of platelets on each VWF string in all subsequent 1200 video frames, and changes in platelet number were plotted in the function of time (supplemental Fig. S2*A*).

Determining the Length of Each VWF String—First, the size of the image was accurately determined by using a calibration slide (Laboratory Imaging Ltd., Prague, Czech Republic). Second, the software used the position of the platelets on the VWF string to calculate the length of the VWF strings by adding up interplatelet distances (distances between the center of the platelets) per VWF string. Hence, the "minimal" length of a VWF string is determined by the position of the first and last platelet bound. The length was calculated for all subsequent 1200 video frames, and changes in VWF string length were plotted in the function of time (supplemental Fig. S2*B*).

Determining Cleavage Site Positions in Each VWF String—Cleavage site positions in the VWF strings were identified by a decrease in both VWF string length (supplemental Fig. S2*A*, *black arrows*) and platelet number (supplemental Fig. S2*B*, *black arrows*). The length of the cleaved fragments was calculated by subtracting the length of the remaining part of the VWF string from the original VWF string length.

RESULTS

VWF Strings Anchored to the Surface of BOECs Are Specifically Removed by ADAMTS13—Processing of VWF strings by ADAMTS13 was studied on the surface of BOECs. These cells are a good alternative for human umbilical vein endothelial cells; they are easily isolated from peripheral blood (19, 20) and are endothelial progenitor cells with all the typical endothelial characteristics, including formation of Weibel-Palade bodies (20, 25). Stimulation of BOECs with histamine resulted in the release of VWF multimers, of which some remained anchored to the surface of the endothelial cells. These VWF multimers were visualized through the binding of fluorescently labeled washed platelets (Fig. 1*A*).

In the first bulk experiment, we determined the disappearance of VWF strings, in the presence or absence of ADAMTS13, by counting the remaining strings in the function of time. In the presence of buffer, 78 ± 4% (n = 3) of the released VWF strings remained attached during the course of the experiment (Fig. 1*B*). Perfusion with recombinant WT

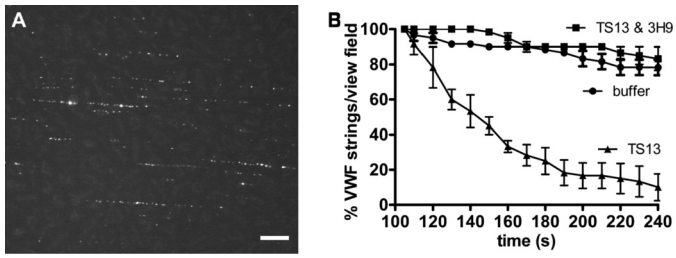

FIGURE 1. **VWF strings on the surface of BOECs are removed by ADAMTS13.** *A*, platelet-decorated VWF strings are visualized by fluorescence microscopy on the surface of BOECs perfused with washed DIOC6-labeled platelets at a shear rate of 250 s^{-1}. Scale bar corresponds to 50 μm. *B*, disappearance of the VWF strings was followed in the function of time in the presence of buffer (●), recombinant WT ADAMTS13 alone (*TS13*, ▲) or with the inhibitory anti-ADAMTS13 mAb 3H9 (*TS13* & 3H9, ■). Data represent the mean ± S.E. (n = 3). In total, 60 strings were analyzed per condition.

ADAMTS13 resulted in the gradual disappearance of VWF strings from the endothelial cell surface (Fig. 1*B*). In 10 ± 8% of the cases, short fragments of VWF strings remained attached to the endothelial surface at the end of the experiment. VWF string processing was ADAMTS13-specific because the addition of the inhibitory anti-ADAMTS13 antibody 3H9 blocked cleavage (Fig. 1*B*) (24). It must be noted that even in the absence of ADAMTS13 or in the presence of both ADAMTS13 and its inhibitory mAb 3H9, a small fraction of VWF strings (22 and 17%, respectively, Fig. 1*B*) disappeared from the endothelial surface, most probably due to the hydrodynamic forces they experience. These data corroborate previous results (12) and demonstrate that BOECs are a good alternative for human umbilical vein endothelial cells to study ADAMTS13-mediated processing of VWF strings on the surface of endothelial cells.

VWF Strings Are Cleaved Multiple Times by ADAMTS13—ADAMTS13-mediated cleavage of VWF strings (n = 40) on the surface of BOECs was next studied in detail using imaging and computing software. VWF string length (= the sum of all interplatelet distances, Fig. 2*A*) and the number of platelets adhering to the string were followed in the function of time (Fig. 2*B*). The stepwise shortening of a VWF string by ADAMTS13 is obvious from the decrease in the calculated VWF string length (Fig. 2*A*, *arrows*) and decrease in the number of attached platelets (Fig. 2*B*, *arrows*). Four internal cleavage events occurred in the representative VWF string depicted in Fig. 2 (Fig. 2, *A* and *B*, *black arrows*, and *C*) before the string was completely removed from the endothelial surface (Fig. 2, *A* and *B*, *open arrows*).

Analysis of the cleavage events in all observed VWF strings (n = 40) demonstrated that the number of internal cleavage events in each VWF string varied from one to up to eight events, with a median of three (Fig. 2*D*). In a minority of cases (8% of all observed strings), the VWF string was not successively shortened by ADAMTS13 but disappeared in its entirety from the endothelial surface (VWF strings undergoing zero internal cleavage events, Fig. 2*D*). Removal of these strings could also include events independent of ADAMTS13 because string disappearance was also observed in the presence of buffer (Fig. 1 and supplemental Fig. S3) and inactive mutant ADAMTS13 E225Q (supplemental Fig. S3), as described in the previous paragraph.

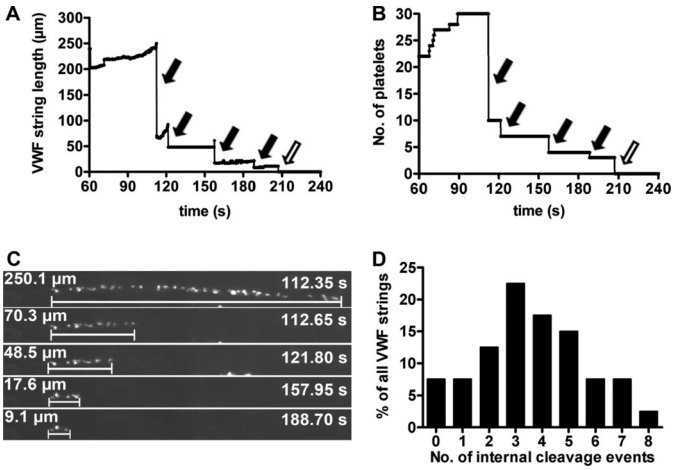

FIGURE 2. **VWF strings are cleaved multiple times.** Individual VWF strings were followed in the function of time in the presence of recombinant ADAMTS13. *A* and *B*, changes in VWF string length (*A*) and the number of adhering platelets (*B*) are depicted for a representative string. This VWF string was successively shortened by four internal cleavage events (*black arrows*) before the remainder of the string disappeared from the endothelial surface (*open arrows*). *C*, the video frames corresponding to the four internal cleavage events depicted in *A* and *B* are shown, with the length of the VWF fragment and the time in the *left-hand* and the *right-hand* corners, respectively. *D*, the number of internal ADAMTS13 cleavage events in 40 VWF strings (from three independent experiments) expressed as a percentage of all strings analyzed. Zero internal cleavage events correspond to VWF strings disappearing in their entirety from the endothelial surface. The disappearance of the remaining portion of VWF strings (*open arrows*) is not represented because only internal cleavage events are shown.

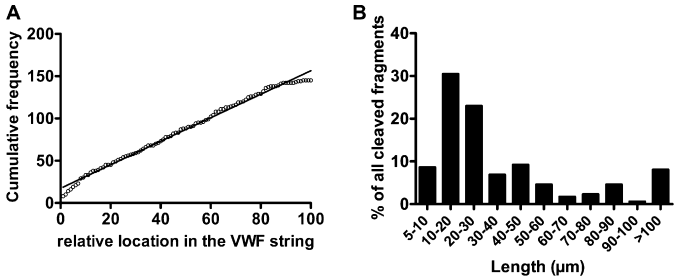

FIGURE 3. **ADAMTS13 cleavage sites are found over the VWF string, generating large VWF fragments.** *A*, the positions of the ADAMTS13 cleavage sites in VWF strings ($n = 40$) were analyzed. Each VWF string was divided in 100 segments of equal length with the beginning of the string (the attachment site to the endothelial cell) corresponding to relative location 1 and the end of the string corresponding to relative location 100. *B*, the length of the VWF proteolytic fragments was calculated by subtracting the length of the VWF portion that remained attached to the endothelial cells after ADAMTS13 proteolysis from the original VWF string length. The distribution of the length of the generated VWF multimers was determined for 40 VWF strings in three independent experiments in the presence of recombinant WT ADAMTS13 and is depicted as the percentage of all fragments measured.

In addition, in the absence of active ADAMTS13, a small number of internal cleavage-like events occurred (supplemental Fig. S3), during which a part of the VWF string disappeared. Although low in number, 29 events (44 strings) in buffer and 24 events (49 strings) in the presence of inactive ADAMTS13, we cannot discriminate these internal cleavage-like events from internal cleavage events (145 in 40 strings) in the presence of active ADAMTS13 depicted in Fig. 2*D*. In conclusion, we show here that successive shortening of the VWF string takes place in the presence of ADAMTS13 in the function of time with multiple cleavage events per string.

ADAMTS13 Cleavage Sites Are Distributed throughout the VWF String Releasing Large VWF Fragments—Because ADAMTS13 cleaves VWF strings multiple times at different sites, cleavage site locations were determined. There was a linear correlation ($R^2 = 0.9927$) between cumulative frequency of the number of cleavage events and the VWF string location, indicating that cleavage sites are evenly distributed throughout the string (Fig. 3*A*). However, in the beginning and at the end of the VWF string, the slope of the curve was more or less steep, respectively, corresponding to a slight increase and decrease in cleavage events when compared with the rest of the string (Fig. 3*A*).

Calculation of the length of VWF multimers released after each cleavage event showed that large VWF fragments were generated after ADAMTS13 proteolysis, ranging in size from 5 μm to up to more than 100 μm (Fig. 3*B*), with a median calculated length of 23 μm. In conclusion, although ADAMTS13 cleavage sites are dispersed over the VWF string, generated VWF fragments are still large in size.

Local Elongation of the VWF String Precedes ADAMTS13-mediated Cleavage—We next carefully studied changes in VWF string length in the function of time in the presence of ADAMTS13. An increase in VWF string length is observed before proteolysis by ADAMTS13 in four out of five cleavage events in the VWF string depicted in Fig. 4 (Fig. 4*A*, *black arrows* with *asterisks*). The same accounts for the string depicted in Fig. 2*A* for three out of the four internal cleavage events (*first three black arrows*). This increase in VWF string length was not due to binding of additional platelets up or downstream of the first and last platelet, respectively, because platelet numbers remained constant during elongation (Fig. 4*B*, *black arrows* with *asterisks*). Interestingly, this increase in VWF string length before cleavage was always associated with a local increase in interplatelet distance exactly at the cleavage site (Fig. 4, *C* and *D*). Increase in interplatelet distances at other sites was also observed (see the last paragraph under "Results"), as evidenced by the often large changes in VWF string length observed (Fig. 4*A*, *second* and *third black arrow*).

Analysis of all cleavage events in the 40 VWF strings analyzed revealed that in 89% of the events, the VWF string elongated at the cleavage site before proteolysis occurred. Because our assay detection limit for elongation is 1.4 μm (the size corresponding to two pixels), it is possible that in the remaining 11% of the cleavage events, smaller but undetectable extensions occur at the cleavage site.

We next measured the length of the increase in interplatelet distance at each cleavage site ($n = 128$ in 40 strings analyzed). Increases in interplatelet distance at the cleavage site varied from 1.4 (detection limit) to 40 μm with a median of 6 μm (Fig. 4*E*). Moreover, there was no correlation between the length of the elongation and the length of the VWF fragment downstream of the cleavage site nor with the number of platelets attached to the VWF fragment downstream of the cleavage site (data not shown). Thus, cleavage of VWF by ADAMTS13 is preceded by a local elongation of the VWF string precisely at the cleavage site.

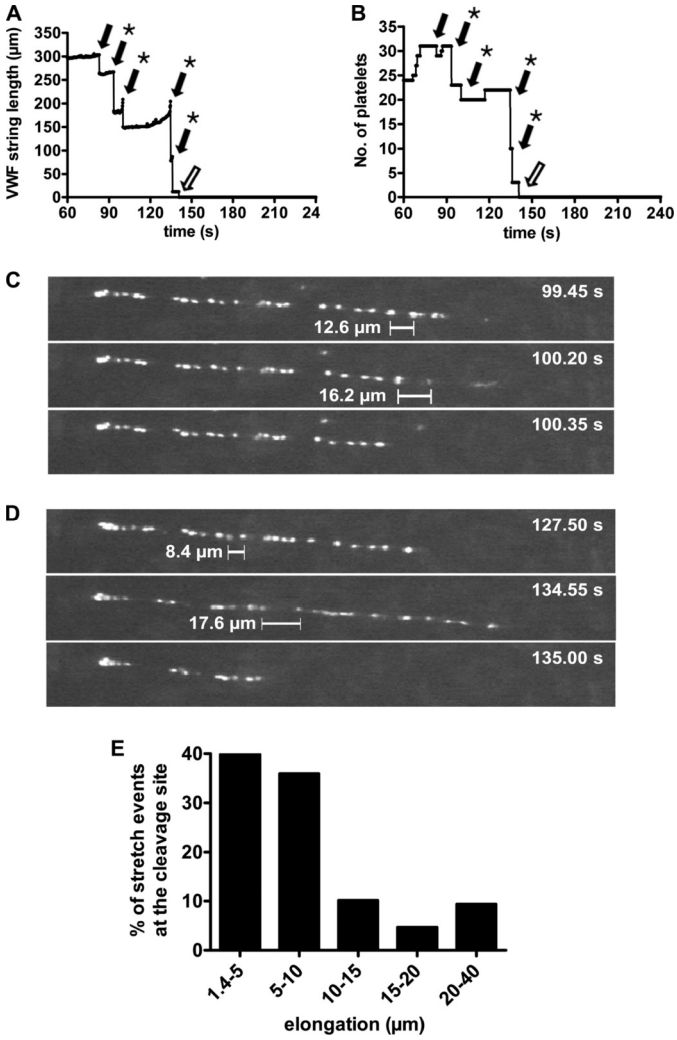

FIGURE 4. **Local elongation of the VWF string precedes ADAMTS13-mediated cleavage.** Changes in VWF string length and platelet number in the presence of recombinant WT ADAMTS13 were followed in the function of time (*A* and *B*, respectively). A representative VWF string of 40 observed strings is shown. Five internal cleavage events occurred in the VWF string (*A* and *B*, *black arrows*) before the last part of the VWF string disappeared from the endothelial surface (*A* and *B*, *open arrows*). An increase in VWF string length was observed at the cleavage site in four out of the five internal cleavage events (*A* and *B*, *black arrows* with *asterisks*). The video frames corresponding to the third and fourth internal cleavage events depicted in *A* are shown in *C* and *D*, respectively. The interplatelet distance is depicted by the *scale bars* with the length of the distance at the cleavage site indicated. The moment of the cleavage event is shown in the *right-hand corner*. *E*, the length of elongations at the cleavage site was determined by calculating the difference in length before and after elongation. The distribution of the length of the elongation is depicted as a percentage of the number of elongation events measured only at the cleavage sites.

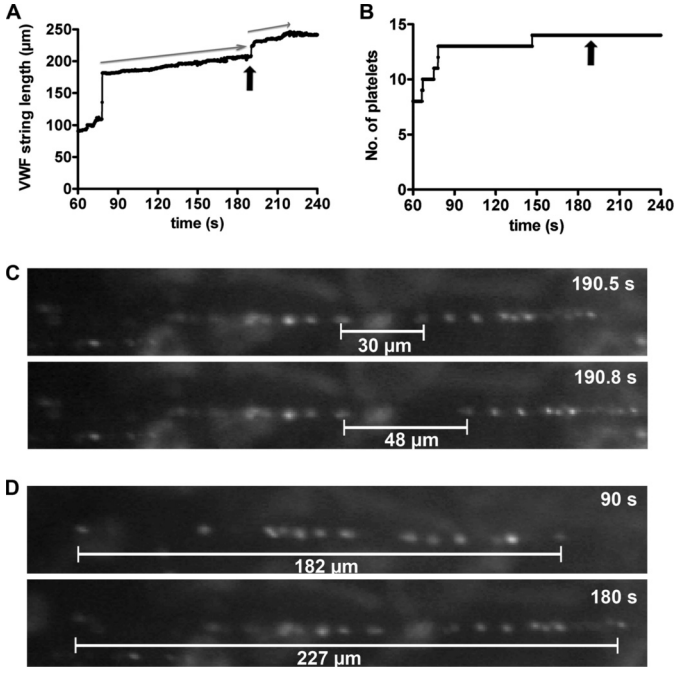

FIGURE 5. **Elongation is a general phenomenon of the VWF string.** Changes in VWF string length and number of attached platelets in the presence of buffer were followed in the function of time (*A* and *B*, respectively). One elongation of >1.4 μm (*A*, *black arrow*) and two gradual increases in VWF string length (*A*, *gray arrows*) were observed in a representative string. The video frames corresponding to the local sudden and the first gradual elongation are depicted in *C* and *D*, respectively. The increase in sudden interplatelet distance (*C*) or gradual VWF string length (*D*) is depicted by the *white bar*, and the length of the observed extension is indicated below. The times of the video frames are shown in the *right-hand corners*. This figure is representative of 44 VWF strings analyzed in three independent experiments.

Local Elongation Is a General Feature of VWF Strings Moving in the Direction of Flow—To investigate whether local elongations were a general feature of VWF strings moving in the direction of flow, we measured all changes in interplatelet distances in VWF strings in the presence of buffer (44 strings) and inactive ADAMTS13 (E225Q) (49 strings) in the function of time. As shown here in the absence of ADAMTS13, elongation was observed as a sudden increase in VWF string length (Fig. 5, *A*, *black arrow*, and *C*) or a gradual increase in VWF string length, resulting from the accumulation of multiple local elongations at different time points (Fig. 5, *A*, *gray arrows*, and *D*). These sudden (Fig. 2*A*, third internal cleavage event; Fig. 4, third and fourth internal cleavage event) and gradual (Fig. 4*A*, second and fourth cleavage event) increases in VWF string length were also observed in the presence of ADAMTS13. These data demonstrate that elongations occur at different sites, random in space and time.

Elongation was detected in 96% ± 3 ($n = 3$) and 91% ± 15 ($n = 3$), respectively, of all VWF strings studied in the presence of inactive ADAMTS13 (E225Q) or buffer. Also, in the presence of active ADAMTS13, 98% ± 4 ($n = 3$) of the strings elongated.

In addition, performing experiments in the presence of buffer or inactive ADAMTS13 (E225Q) allowed us to determine the length of intact VWF multimers attached to the surface of endothelial cells. VWF strings could reach lengths up to 500 μm with a median of 108 μm (supplemental Fig. S4). Longer VWF strings also had more platelets bound to them (Pearson coefficient 0.82, data not shown). In conclusion, VWF multimers attached to endothelial cells and moving in the direction of flow experience local elongations at different sites, independent of the presence of ADAMTS13.

Large Elongations Occur throughout the VWF String—The length of all local elongations in VWF strings in the presence of buffer, inactive ADAMTS13, and active ADAMTS13 was measured to get insight into the size distribution of all observed extensions. The length distribution of all local elongations ranged from 1.4 (detection limit) to 40 μm with a median of 2.8

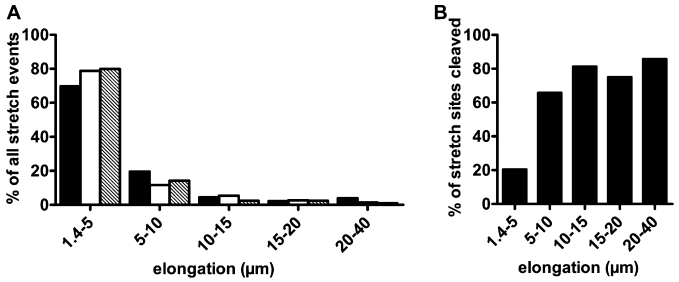

FIGURE 6. **Large local elongations occur throughout the VWF string.** *A*, the length of all elongations occurring in the VWF string was determined by calculating the difference in length before and after extension. The distribution of the length of the elongation is depicted as a percentage of the number of elongation events measured, in the presence of buffer (44 strings in three experiments) (*open bars*), active ADAMTS13 (40 strings in three experiments) (*filled bars*), and inactive ADAMTS13 (E225Q) (49 strings in three experiments) (*hatched bars*). *B*, the percentage of elongated sites cleaved in each length category.

μm and was the same in the presence of recombinant WT ADAMTS13, buffer, or inactive ADAMTS13 (E225Q) (Fig. 6*A*).

In addition, the length distribution of the elongations at the cleavage site (Fig. 4*E*) differed from the length distribution of all elongations (Fig. 6*A*). Of the 352 elongation events observed in the presence of ADAMTS13, 128 were associated with cleavage. Elongations with a length larger than 5 μm were cleaved in 66–86% of the cases, whereas only 20% of the stretches with a length between 1.4 and 5 μm were cleaved (Fig. 6*B*).

In conclusion, large elongations occur between two adjacent platelets at different sites in the VWF string. Under the current experimental conditions, 36% of these sites were cleaved by ADAMTS13.

DISCUSSION

In this study, we examined the cleavage of VWF strings by ADAMTS13 using imaging and computing software to gain insight into the number, location, and characteristics of the ADAMTS13 cleavage sites. We showed that platelet-decorated VWF strings are cleaved multiple times by ADAMTS13, successively shortening the VWF string in the function of time. In this way, VWF fragments of different sizes are generated that are, however, still ultra-large. Interestingly, local elongations occur in VWF strings, and these are the preferred sites for ADAMTS13 cleavage.

Previous analysis of ADAMTS13-mediated processing of VWF strings suggested that strings are generally digested one or two times close to the upstream attachment site (12). We show here, however, that VWF strings are gradually digested multiple times in the function of time and that cleavage sites are evenly distributed throughout the VWF string and not restricted to the region close to the upstream attachment sites. The VWF fragments generated after proteolysis of the VWF strings were still large in size, varying from 5 to over 100 μm. This implies that the released VWF fragments, if fully extended, still consist of 85 to more than 1000 monomers (with the length of one monomer ~60 nm (26)). Hence, cleaved VWF fragments have lengths larger than those of plasma VWF (40 monomers (4, 26)). This is in agreement with data from Jin. *et al.* (27), who demonstrated, using multimer analysis, that cleavage of EC-anchored VWF (both in the presence and in the absence of shear) resulted in VWF fragments that were still ultra-large in size. Further proteolysis of VWF multimers to obtain multimers with sizes of those found in plasma is likely to occur in circulation. Recently, it was predicted that VWF multimers consisting of more than 200 monomers are prone to digestion by ADAMTS13 in circulation (28). Moreover, the presence of platelets might increase ADAMTS13 cleavage of VWF in solution (29).

In the absence of ADAMTS13, we observed both detaching of VWF strings in their entirety from the endothelial surface and shortening of the VWF strings. We defined the latter as cleavage-like events because they occurred in the absence of exogenously added ADAMTS13. It is rather unlikely that ADAMTS13 present in platelets (30) and endothelial cells (18) is responsible for the removal or shortening of the VWF strings because cleavage by endothelium-derived ADAMTS13 was only observed under static conditions when the amount of ADAMTS13 was allowed to accumulate (18). It is more likely that the disappearance or shortening of the VWF strings in the absence of ADAMTS13 is attributed to the mechanical breaking of self-associated VWF strings (14, 31–33).

Intriguingly, micrometer-scale analysis showed that elongation of the VWF string preceded ADAMTS13 proteolysis. However, elongation was not observed at all cleavage sites (89%), probably due to the detection limit of our assay as only elongations larger than 1.4 μm (corresponding to ~20 monomers) could be detected. In addition, elongation of the VWF string did not only occur at the cleavage sites but also at other sites without subsequent cleavage by ADAMTS13. The fact that not all elongated sites were cleaved might be due to the low physiological concentration of ADAMTS13 used. On the other hand, cleavage sites might also be shielded by VWF-binding proteins such as thrombospondine-1 (34, 35) or osteoprotegerin secreted by platelets or EC (36), respectively.

Local elongation of VWF strings occurred at different sites, independent of the presence of ADAMTS13, showing that this phenomenon is a characteristic behavior of most VWF strings under flow. Analyzing the length of the elongations demonstrated that VWF strings could elongate (locally) up to 40 μm, with a median of 2.8 μm. If the observed stretches would represent fully extended parts in the VWF multimer, then a stretch of 2.8 μm would cover ~50 monomers (one monomer is 60 nm) (26). The occurrence of such large elongations at different sites might imply that the quaternary structure of a VWF string anchored to an endothelial cell still contains condensed regions, although these strings largely unfurl upon release from Weibel-Palade bodies. In fact, VWF multimers are packed as constrained springs in tubules in the Weibel-Palade bodies to prevent entanglement and allow formation of VWF strings. At release, changes in pH weaken these constraints and allow unfurling of VWF, probably aided by flow (37, 38). We hypothesize that certain parts in the exocytosed VWF string are still more constrained than others. Further local unfurling of the VWF string in the direction of the flow results in local elongation, which exposes multiple exosites for ADAMTS13 simultaneously. Furthermore, preferentially, elongations larger than 5 μm are cleaved by ADAMTS13. This might be due to the fact

that many more exosites might become exposed in these larger elongations, increasing the chance of cleavage by ADAMTS13.

Recently, Huang *et al.* (14) demonstrated that both platelet-decorated and platelet-free VWF multimers were anchored to the surface of endothelial cells. The software program used here only studies changes in VWF string length of the platelet-decorated VWF strings as changes in length of the VWF string are calculated based on the position of the platelets. Once the *in vivo* relevance of platelet-free VWF strings has been determined, these VWF strings can be detected with fluorescently labeled anti-VWF antibodies (14), and changes in length will then be studied with an adapted software program.

In conclusion, we observed an exocytosed VWF string with bound platelets that further elongates in the direction of the flow. Large elongations (>2 μm) occur at certain sites and involve 20 to more than 500 monomers, if fully extended, implying that at these sites in the VWF string, multiple ADAMTS13 exosites and cleavage sites in the VWF A2 domains might become exposed simultaneously. These regions are hence susceptible for ADAMTS13-mediated cleavage. Thus, elongation might increase the exposure of ADAMTS13 exosites in the VWF string and provide a mechanism for the rapid cleavage of prothrombotic EC-anchored UL-VWF strings.

Acknowledgment—We thank H. Pottel (Laboratory for Biophysics K.U.Leuven, Campus Kortrijk) for help with statistical analysis.

REFERENCES

1. Sadler, J. E. (1998) *Annu. Rev. Biochem.* **67,** 395–424
2. Sadler, J. E. (2005) *J. Thromb. Haemost.* **3,** 1702–1709
3. Ruggeri, Z. M. (2003) *Curr. Opin. Hematol* **10,** 142–149
4. De Meyer, S. F., Deckmyn, H., and Vanhoorelbeke, K. (2009) *Blood* **113,** 5049–5057
5. Sporn, L. A., Marder, V. J., and Wagner, D. D. (1986) *Cell* **46,** 185–190
6. Moake, J. L., Rudy, C. K., Troll, J. H., Weinstein, M. J., Colannino, N. M., Azocar, J., Seder, R. H., Hong, S. L., and Deykin, D. (1982) *N. Engl. J. Med.* **307,** 1432–1435
7. Tsai, H. M. (2007) *Hematol. Oncol. Clin. North Am.* **21,** 609–632
8. Feys, H. B., Liu, F., Dong, N., Pareyn, I., Vauterin, S., Vandeputte, N., Noppe, W., Ruan, C., Deckmyn, H., and Vanhoorelbeke, K. (2006) *J. Thromb. Haemost.* **4,** 955–962
9. Levy, G. G., Nichols, W. C., Lian, E. C., Foroud, T., McClintick, J. N., McGee, B. M., Yang, A. Y., Siemieniak, D. R., Stark, K. R., Gruppo, R., Sarode, R., Shurin, S. B., Chandrasekaran, V., Stabler, S. P., Sabio, H., Bouhassira, E. E., Upshaw, J. D., Jr., Ginsburg, D., and Tsai, H. M. (2001) *Nature* **413,** 488–494
10. Tsai, H. M. (1996) *Blood* **87,** 4235–4244
11. Furlan, M., Robles, R., and Lämmle, B. (1996) *Blood* **87,** 4223–4234
12. Dong, J. F., Moake, J. L., Nolasco, L., Bernardo, A., Arceneaux, W., Shrimpton, C. N., Schade, A. J., McIntire, L. V., Fujikawa, K., and López, J. A. (2002) *Blood* **100,** 4033–4039
13. Motto, D. G., Chauhan, A. K., Zhu, G., Homeister, J., Lamb, C. B., Desch, K. C., Zhang, W., Tsai, H. M., Wagner, D. D., and Ginsburg, D. (2005) *J. Clin. Invest.* **115,** 2752–2761
14. Huang, J., Roth, R., Heuser, J. E., and Sadler, J. E. (2009) *Blood* **113,** 1589–1597
15. Padilla, A., Moake, J. L., Bernardo, A., Ball, C., Wang, Y., Arya, M., Nolasco, L., Turner, N., Berndt, M. C., Anvari, B., López, J. A., and Dong, J. F. (2004) *Blood* **103,** 2150–2156
16. Chauhan, A. K., Goerge, T., Schneider, S. W., and Wagner, D. D. (2007) *J. Thromb. Haemost.* **5,** 583–589
17. Turner, N., Nolasco, L., Dong, J. F., and Moake, J. (2009) *J. Thromb. Haemost.* **7,** 229–232
18. Turner, N. A., Nolasco, L., Ruggeri, Z. M., and Moake, J. L. (2009) *Blood* **114,** 5102–5111
19. Lin, Y., Chang, L., Solovey, A., Healey, J. F., Lollar, P., and Hebbel, R. P. (2002) *Blood* **99,** 457–462
20. De Meyer, S. F., Vanhoorelbeke, K., Chuah, M. K., Pareyn, I., Gillijns, V., Hebbel, R. P., Collen, D., Deckmyn, H., and VandenDriessche, T. (2006) *Blood* **107,** 4728–4736
21. Feys, H. B., Anderson, P. J., Vanhoorelbeke, K., Majerus, E. M., and Sadler, J. E. (2009) *J. Thromb. Haemost.* **7,** 2088–2095
22. Anderson, P. J., Kokame, K., and Sadler, J. E. (2006) *J. Biol. Chem.* **281,** 850–857
23. Feys, H. B., Pareyn, I., Vancraenenbroeck, R., De Maeyer, M., Deckmyn, H., Van Geet, C., and Vanhoorelbeke, K. (2009) *Blood* **114,** 4749–4752
24. Feys, H. B., Roodt, J., Vandeputte, N., Pareyn, I., Lamprecht, S., van Rensburg, W. J., Anderson, P. J., Budde, U., Louw, V. J., Badenhorst, P. N., Deckmyn, H., and Vanhoorelbeke, K. (2010) *Blood* **116,** 2005–2010
25. van den Biggelaar, M., Bouwens, E. A., Kootstra, N. A., Hebbel, R. P., Voorberg, J., and Mertens, K. (2009) *Haematologica* **94,** 670–678
26. Fowler, W. E., Fretto, L. J., Hamilton, K. K., Erickson, H. P., and McKee, P. A. (1985) *J. Clin. Invest.* **76,** 1491–1500
27. Jin, S. Y., Skipwith, C. G., Shang, D., and Zheng, X. L. (2009) *J. Thromb. Haemost.* **7,** 1749–1752
28. Zhang, X., Halvorsen, K., Zhang, C. Z., Wong, W. P., and Springer, T. A. (2009) *Science* **324,** 1330–1334
29. Shim, K., Anderson, P. J., Tuley, E. A., Wiswall, E., and Sadler, J. E. (2008) *Blood* **111,** 651–657
30. Suzuki, M., Murata, M., Matsubara, Y., Uchida, T., Ishihara, H., Shibano, T., Ashida, S., Soejima, K., Okada, Y., and Ikeda, Y. (2004) *Biochem. Biophys. Res. Commun.* **313,** 212–216
31. Savage, B., Sixma, J. J., and Ruggeri, Z. M. (2002) *Proc. Natl. Acad. Sci. U.S.A.* **99,** 425–430
32. Ulrichts, H., Vanhoorelbeke, K., Girma, J. P., Lenting, P. J., Vauterin, S., and Deckmyn, H. (2005) *J. Thromb. Haemost.* **3,** 552–561
33. Li, Y., Choi, H., Zhou, Z., Nolasco, L., Pownall, H. J., Voorberg, J., Moake, J. L., and Dong, J. F. (2008) *J. Thromb. Haemost.* **6,** 1135–1143
34. Wang, A., Liu, F., Dong, N., Ma, Z., Zhang, J., Su, J., Zhao, Y., and Ruan, C. (2010) *Thromb. Res.* **126,** e260–e265
35. Bonnefoy, A., Daenens, K., Feys, H. B., De Vos, R., Vandervoort, P., Vermylen, J., Lawler, J., and Hoylaerts, M. F. (2006) *Blood* **107,** 955–964
36. Zannettino, A. C., Holding, C. A., Diamond, P., Atkins, G. J., Kostakis, P., Farrugia, A., Gamble, J., To, L. B., Findlay, D. M., and Haynes, D. R. (2005) *J. Cell Physiol.* **204,** 714–723
37. Huang, R. H., Wang, Y., Roth, R., Yu, X., Purvis, A. R., Heuser, J. E., Egelman, E. H., and Sadler, J. E. (2008) *Proc. Natl. Acad. Sci. U.S.A.* **105,** 482–487
38. Michaux, G., Abbitt, K. B., Collinson, L. M., Haberichter, S. L., Norman, K. E., and Cutler, D. F. (2006) *Dev. Cell* **10,** 223–232